上节课回顾

浅水方程

$$\frac{\mathrm{D}\boldsymbol{u}}{\mathrm{D}t} + \boldsymbol{f} \times \boldsymbol{u} = -g\nabla\eta \,,$$

$$\frac{\mathrm{D}h}{\mathrm{D}t} + h\nabla \cdot \boldsymbol{u} = 0 \,.$$

在热带，f 较小

$$\frac{\partial u'}{\partial t} - f_0 v' = -g\frac{\partial \eta'}{\partial x},$$

$$\frac{\partial v'}{\partial t} + f_0 u' = -g\frac{\partial \eta'}{\partial y},$$

$$\frac{\partial \eta'}{\partial t} + H\left(\frac{\partial u'}{\partial x} + \frac{\partial v'}{\partial y}\right) = 0.$$

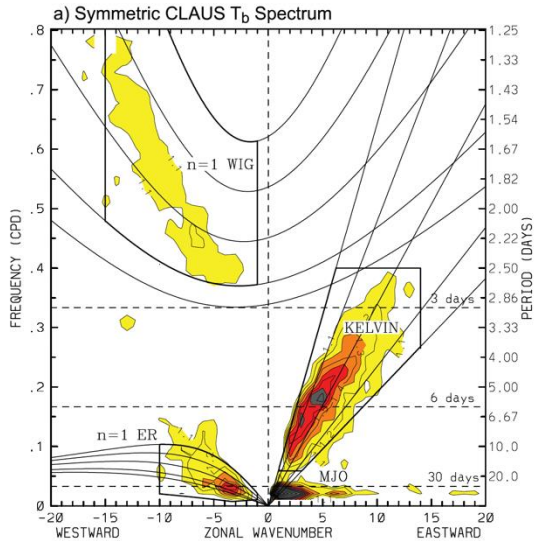

1.4 准地转模型及应用实例

Geostrophic Scaling

$$\frac{\partial \boldsymbol{u}}{\partial t} + \boldsymbol{u} \cdot \nabla \boldsymbol{u} + \boldsymbol{f} \times \boldsymbol{u} = -g \nabla \eta,$$

$$\frac{U}{T} \qquad \frac{U^2}{L} \qquad fU \qquad\qquad g\frac{\mathcal{H}}{L},$$

$$\boxed{Ro\left[\frac{\partial \hat{\boldsymbol{u}}}{\partial \hat{t}} + (\hat{\boldsymbol{u}} \cdot \nabla)\hat{\boldsymbol{u}}\right] + \hat{\boldsymbol{f}} \times \hat{\boldsymbol{u}} = -\nabla \hat{\eta}},$$

$$\psi = (g/f_0)\eta, \qquad \zeta = (g/f_0)\nabla^2 \eta.$$

Conservation of potential vorticity

$$(\boldsymbol{u}\cdot\nabla)\boldsymbol{u} = \frac{1}{2}\nabla(\boldsymbol{u}\cdot\boldsymbol{u}) - \boldsymbol{u}\times(\nabla\times\boldsymbol{u}),$$

Effects of rotation

In a rotating frame of reference, the shallow water momentum equation is

$$\frac{\mathrm{D}\boldsymbol{u}}{\mathrm{D}t} + \boldsymbol{f}\times\boldsymbol{u} = -g\nabla\eta, \tag{3.75}$$

where (as before) $\boldsymbol{f} = f\mathbf{k}$. This may be written in vector invariant form as

$$\frac{\partial\boldsymbol{u}}{\partial t} + (\boldsymbol{\omega}^* + \boldsymbol{f})\times\boldsymbol{u} = -\nabla\left(g\eta + \frac{1}{2}\boldsymbol{u}^2\right), \tag{3.76}$$

Similar to conservation of angular momentum

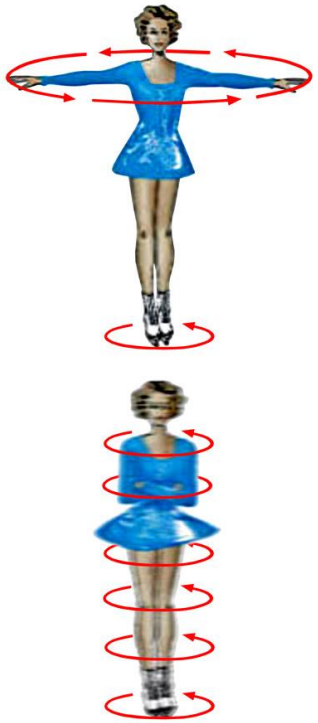

$$\nabla\times(\boldsymbol{\omega}^*\times\boldsymbol{u}) = (\boldsymbol{u}\cdot\nabla)\boldsymbol{\omega}^* - (\boldsymbol{\omega}^*\cdot\nabla)\boldsymbol{u} + \boldsymbol{\omega}^*\nabla\cdot\boldsymbol{u} - \boldsymbol{u}\nabla\cdot\boldsymbol{\omega}^*$$
$$= (\boldsymbol{u}\cdot\nabla)\boldsymbol{\omega}^* + \boldsymbol{\omega}^*\nabla\cdot\boldsymbol{u},$$

and taking the curl of this gives the vorticity equation

$$\frac{\partial\zeta}{\partial t} + (\boldsymbol{u}\cdot\nabla)(\zeta + f) = -(f+\zeta)\nabla\cdot\boldsymbol{u}. \tag{3.77}$$

This is the same as the shallow water vorticity equation in a non-rotating frame, save that ζ is replaced by $\zeta + f$, the reason for this being that f is the vorticity that the fluid has by virtue of the background rotation. Thus, (3.77) is simply the equation of motion for the total or absolute vorticity, $\boldsymbol{\omega}_a = \boldsymbol{\omega}^* + \boldsymbol{f} = (\zeta + f)\mathbf{k}$.

The potential vorticity equation in the rotating case follows, much as in the non-rotating case, by combining (3.77) with the mass conservation equation, giving

$$\boxed{\frac{\mathrm{D}}{\mathrm{D}t}\left(\frac{\zeta + f}{h}\right) = 0}. \tag{3.78}$$

That is, $Q \equiv (\zeta + f)/h$, the potential vorticity in a rotating shallow system, is a material invariant.

$$\boxed{\frac{\mathrm{D}}{\mathrm{D}t}\left(\frac{\zeta + f}{h}\right) = 0}.$$

$$\downarrow$$

$$q = \beta y + \zeta - f_0 \frac{\eta'}{H}$$

$$\downarrow \quad \psi = (g/f_0)\eta,$$

$$\zeta = (g/f_0)\nabla^2 \eta.$$

$$\downarrow$$

$$\boxed{\frac{\mathrm{D}}{\mathrm{D}t}\left(\nabla^2 \psi + \beta y - \frac{1}{L_d^2}\psi\right) = 0},$$

$$\boxed{\frac{\mathrm{D}}{\mathrm{D}t}\left(\nabla^2\psi + \beta y - \frac{1}{L_d^2}\psi\right) = 0},$$

where $\psi = (g/f_0)\eta$, $L_d^2 = gH/f_0^2$, and the advective derivative is

$$\frac{\mathrm{D}}{\mathrm{D}t} = \frac{\partial}{\partial t} + u_g\frac{\partial}{\partial x} + v_g\frac{\partial}{\partial y} = \frac{\partial}{\partial t} - \frac{\partial\psi}{\partial y}\frac{\partial}{\partial x} + \frac{\partial\psi}{\partial x}\frac{\partial}{\partial y} = \frac{\partial}{\partial t} + J(\psi,\cdot). \tag{5.67}$$

$$\boxed{q \equiv \zeta + \beta y - \frac{f_0}{H}\eta = \nabla^2\psi + \beta y - \frac{1}{L_d^2}\psi} \tag{5.69}$$

is the *shallow water quasi-geostrophic potential vorticity.*

$$\frac{\mathrm{D}}{\mathrm{D}t}(\zeta + f - \psi/L_d^2) = 0,$$

忽略第三项

$$\frac{\mathrm{D}}{\mathrm{D}t}(\zeta + \beta y) = 0.$$

$$\psi = \Psi + \psi'(x, y, t), \quad \Psi = -Uy$$

$$\psi' = \mathrm{Re}\,\tilde{\psi}\,\mathrm{e}^{\mathrm{i}(kx+ly-\omega t)},$$

$$\frac{\partial}{\partial t}\nabla^2\psi' + U\frac{\partial \nabla^2\psi'}{\partial x} + \beta\frac{\partial \psi'}{\partial x} = 0.$$

$$\omega = Uk - \frac{\beta k}{K^2}.$$

$$c_p^x \equiv \frac{\omega}{k} = U - \frac{\beta}{K^2}, \qquad c_g^x \equiv \frac{\partial \omega}{\partial k} = U + \frac{\beta(k^2 - l^2)}{(k^2 + l^2)^2}.$$

Mechanism of Rossby Waves

$$\frac{\mathrm{D}}{\mathrm{D}t}(\zeta + \beta y) = 0.$$

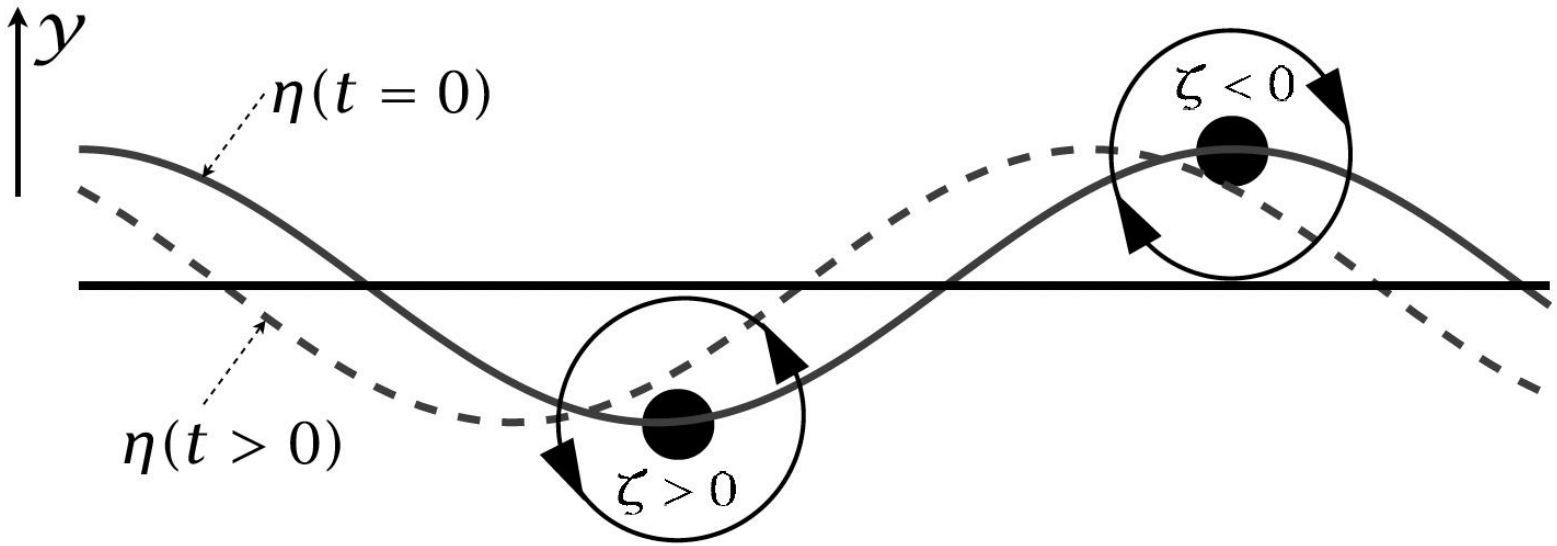

Fig. 5.4 The mechanism of a two-dimensional (x–y) Rossby wave. An initial disturbance displaces a material line at constant latitude (the straight horizontal line) to the solid line marked $\eta(t = 0)$. Conservation of potential vorticity, $\beta y + \zeta$, leads to the production of relative vorticity, as shown for two parcels. The associated velocity field (arrows on the circles) then advects the fluid parcels, and the material line evolves into the dashed line. The phase of the wave has propagated westwards.

Barotropic Instability

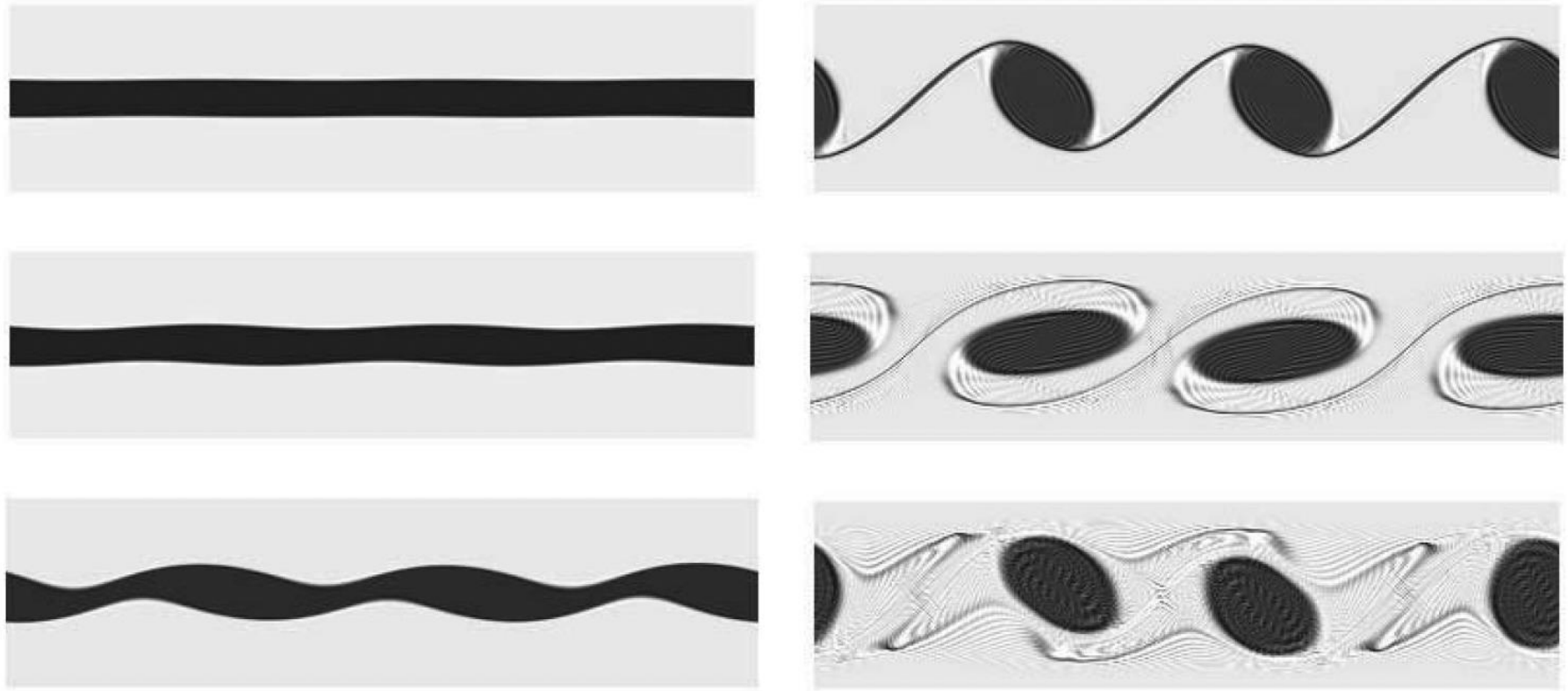

black color represents vorticity

Theoretical results

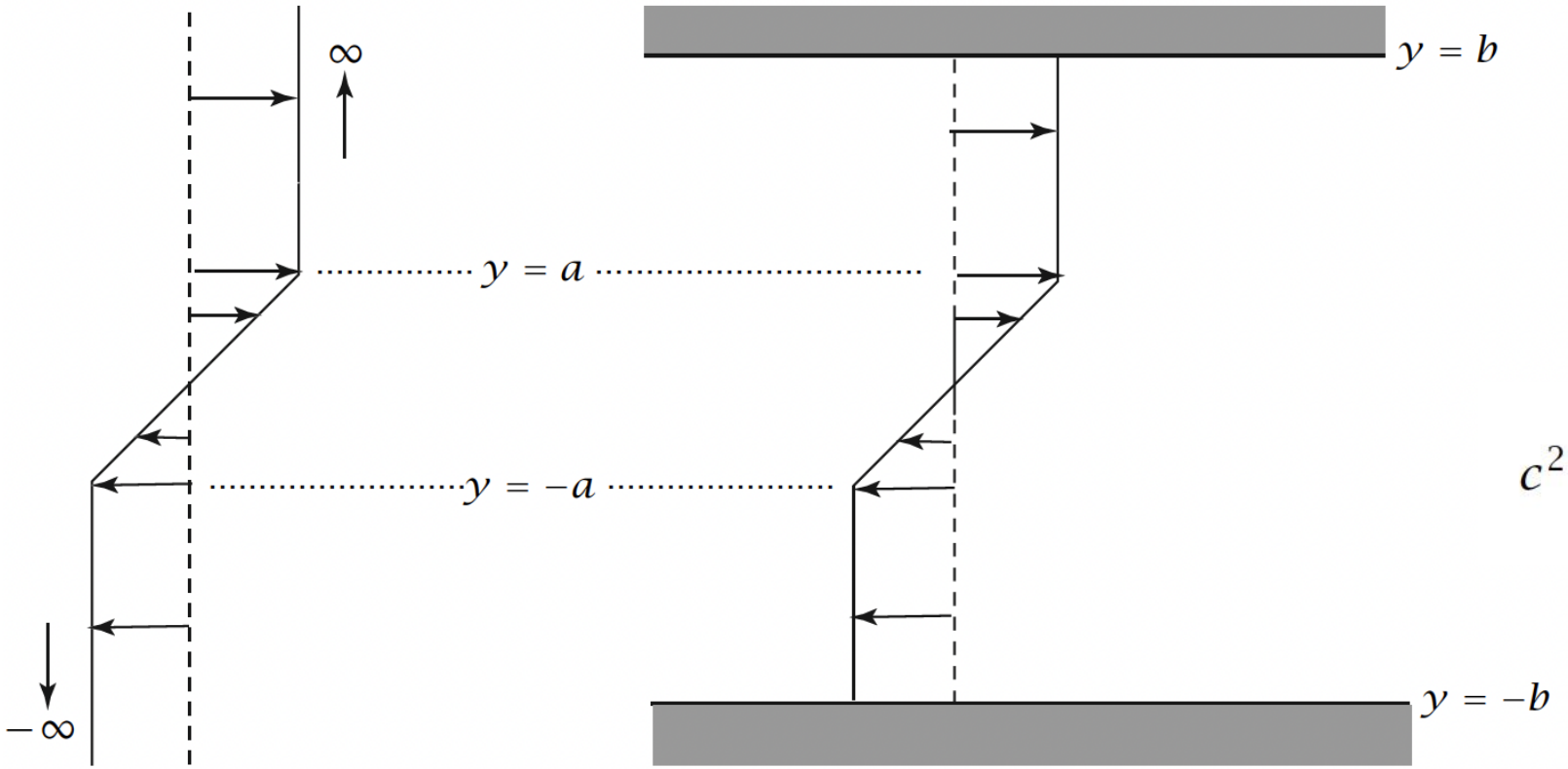

$$\psi' = \mathrm{Re}\,\tilde{\psi}(y)\,\mathrm{e}^{\mathrm{i}k(x-ct)}.$$

$$c^2 = \left(\frac{U_0}{2ka}\right)^2 \left[(1-2ka)^2 - \mathrm{e}^{-4ka}\right],$$

Fig. 6.4 Barotropically unstable velocity profiles. In the simplest case, on the left, a region of shear is sandwiched between two infinite regions of constant velocity. The edge waves at $y = \pm a$ interact to produce an instability. If $a = 0$, then the situation corresponds to that of Fig. 6.1, giving Kelvin–Helmholtz instability. In the case on the right, the flow is bounded at $y = \pm b$. It may be shown that the flow is still unstable, provided that b is sufficiently larger than a. If $b = a$ (plane Couette flow) the flow is stable to infinitesimal disturbances.

Numerically Solving QG equation

$$\frac{\mathrm{D}}{\mathrm{D}t}\left(\nabla^2\psi + \beta y - \frac{1}{L_d^2}\psi\right) = 0$$

$$\frac{\mathrm{D}_0}{\mathrm{D}\hat{t}}(\nabla^2\hat{\psi}_0 + \hat{\beta}\hat{y} - \hat{f}_0^2 F\hat{\psi}_0) = 0,$$

$$\frac{\mathrm{D}}{\mathrm{D}t} = \frac{\partial}{\partial t} - \frac{\partial\psi}{\partial y}\frac{\partial}{\partial x} + \frac{\partial\psi}{\partial x}\frac{\partial}{\partial y}$$

$$\boxed{\frac{D}{Dt}(\nabla^2\psi - f^2 F\psi) + \beta\psi_x = 0}$$

Assume periodic boundary conditions for ψ

Discrete Fourier Transform (DFT)

Discrete Fourier transform

$$X_k = \sum_{n=0}^{N-1} x_n \cdot e^{-i 2\pi \frac{k}{N} n} \qquad \textbf{(Eq.1)}$$

Eq.1 can also be evaluated outside the domain $k \in [0, N-1]$, and that extended sequence is N-periodic. Accordingly, other sequences of N indices are sometimes used, such as $\left[-\frac{N}{2}, \frac{N}{2}-1\right]$ (if N is even) and $\left[-\frac{N-1}{2}, \frac{N-1}{2}\right]$ (if N is odd), which amounts to swapping the left and right halves of the result of the transform.[5]

Inverse transform

$$x_n = \frac{1}{N} \sum_{k=0}^{N-1} X_k \cdot e^{i 2\pi \frac{k}{N} n} \qquad \textbf{(Eq.2)}$$

non-linearities, de-aliased

- assume you need to evaluate DFT($\rho_i u_i$), having given the Fourier transforms ρ_j^* and u_j^*:

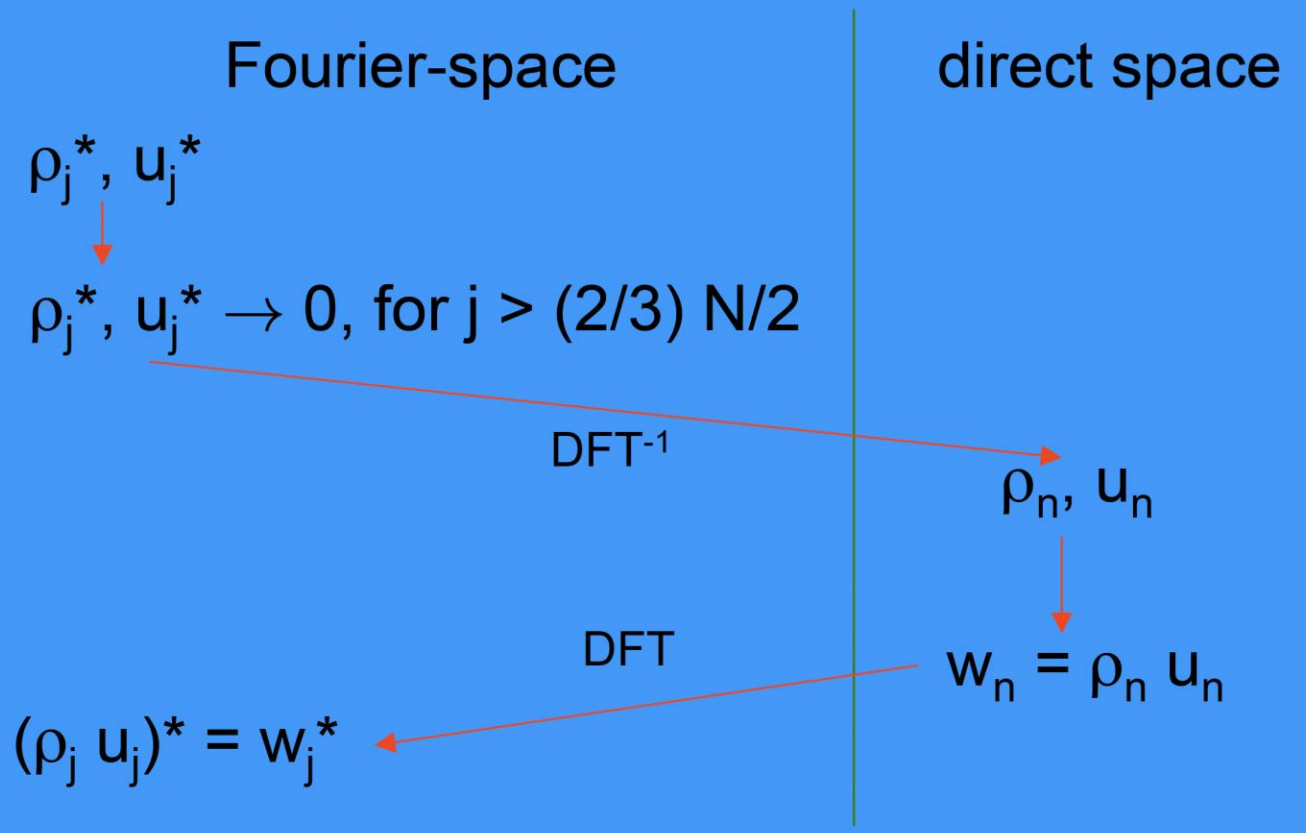

Aliasing

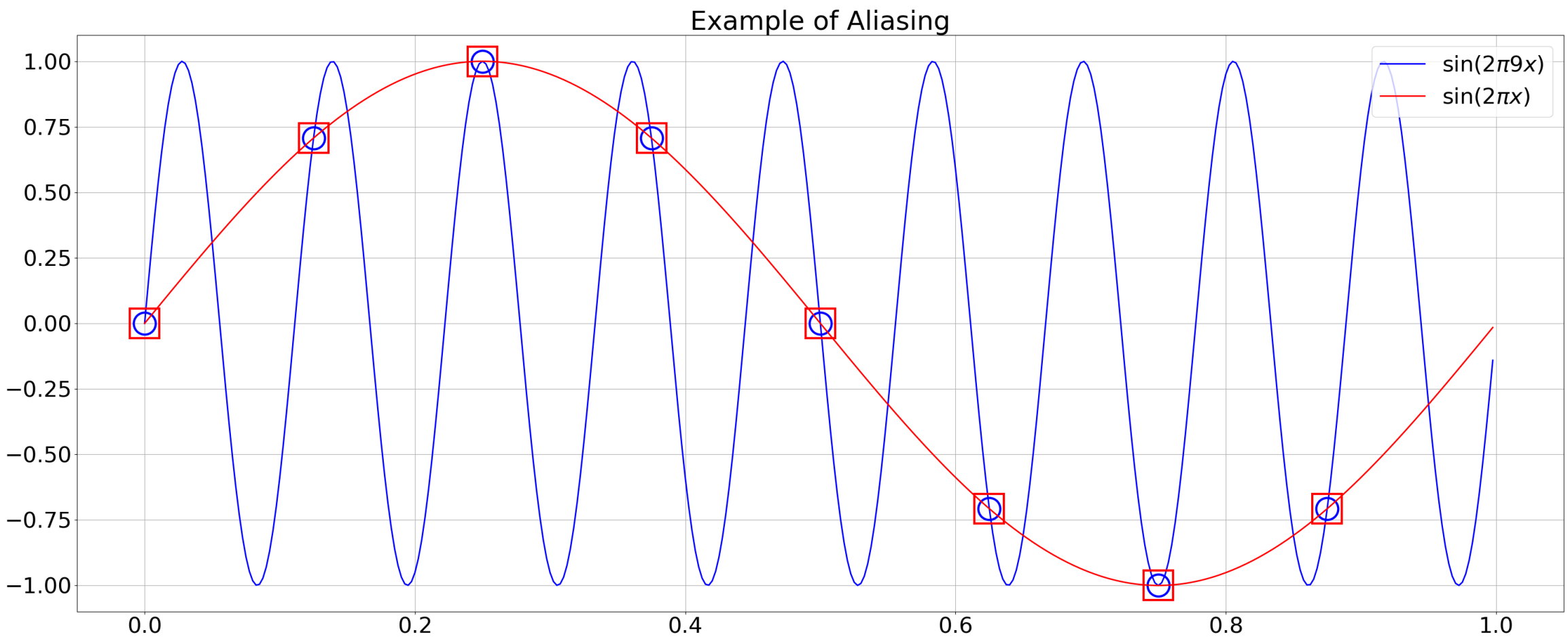
Example of Aliasing
sin(2π9x)
sin(2πx)
1.00
0.75
0.50
0.25
0.00
−0.25
−0.50
−0.75
−1.00
0.0
0.2
0.4
0.6
0.8
1.0

Equation (2.29) is a specific example of the *oscillation equation*

$$\frac{d\psi}{dt} = i\kappa\psi, \tag{2.30}$$

Single-Stage Two-Level Scheme

$$\phi^{n+1} = \phi^n + \Delta t \left(\alpha F(\phi^n) + \beta F(\phi^{n+1})\right), \tag{2.34}$$

$$(1 - i\beta\kappa\Delta t)\phi^{n+1} = (1 + i\alpha\kappa\Delta t)\phi^n.$$

$$\begin{aligned} |A|^2 &= \frac{1 + \alpha^2\kappa^2\Delta t^2}{1 + \beta^2\kappa^2\Delta t^2} \\ &= 1 + (\alpha^2 - \beta^2)\frac{\kappa^2\Delta t^2}{1 + \beta^2\kappa^2\Delta t^2}. \end{aligned}$$

The scheme is stable if alpha <= beta. Need implicit scheme!

Runge–Kutta 2

$$q_1 = hF(\phi^n), \qquad \phi_1 = \phi^n + q_1$$
$$q_2 = hF(\phi_1) - q_1, \quad \phi^{n+1} = \phi_1 + q_2/2$$

Runge–Kutta 4

$$q_1 = hF(\phi^n), \qquad q_2 = hF(\phi^n + q_1/2)$$
$$q_3 = hF(\phi^n + q_2/2), \qquad q_4 = hF(\phi^n + q_3)$$
$$\phi^{n+1} = \phi^n + (q_1 + 2q_2 + 2q_3 + q_4)/6$$

Stability Region of Runge-Kutta Method

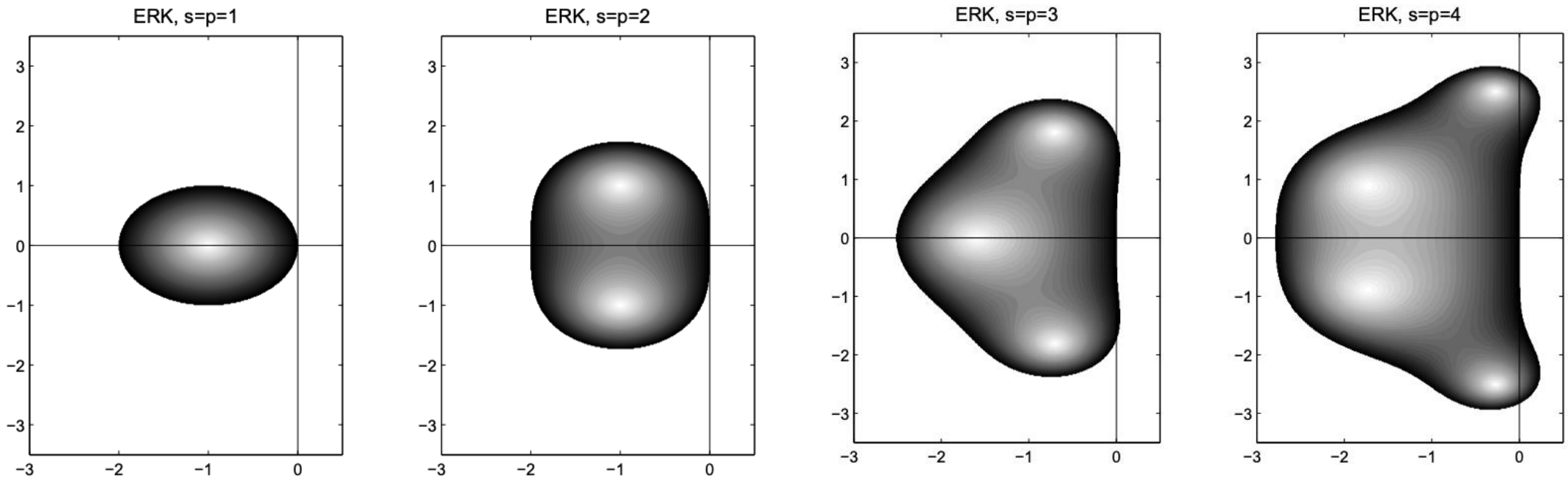

Figure 10.4: Explicit Runge-Kutta Stability Regions

Hyperviscosity

$$-\Delta^2 u \sim -(k^2 + l^2)^2 \tilde{u}$$

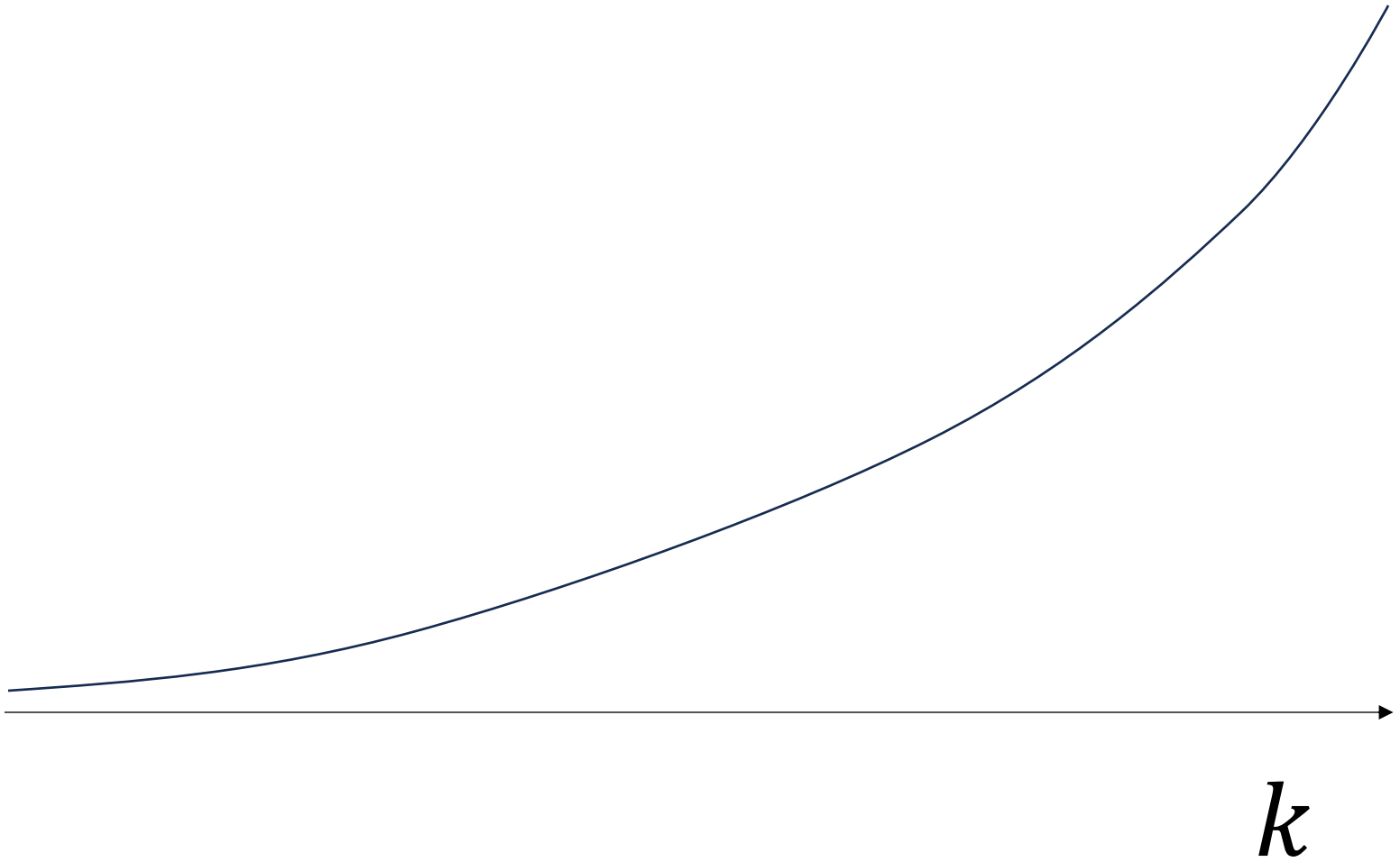

Example 1

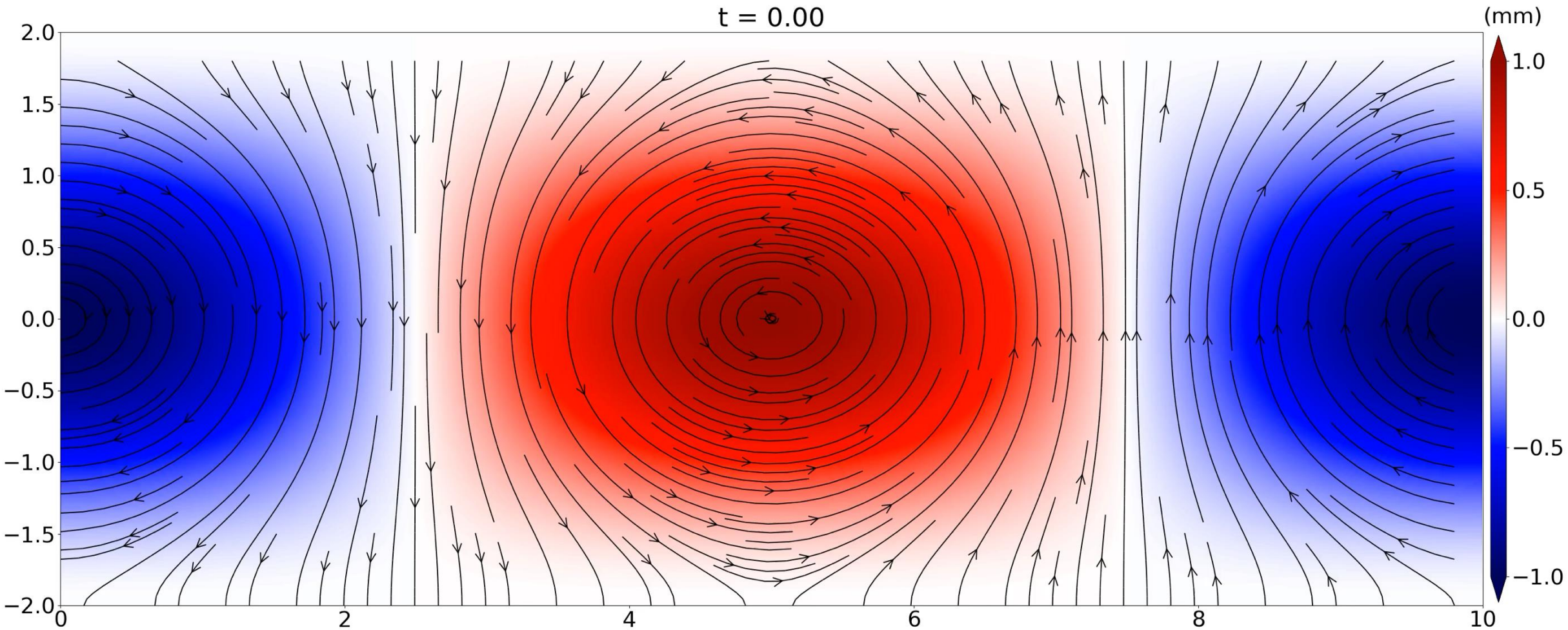

Example 2

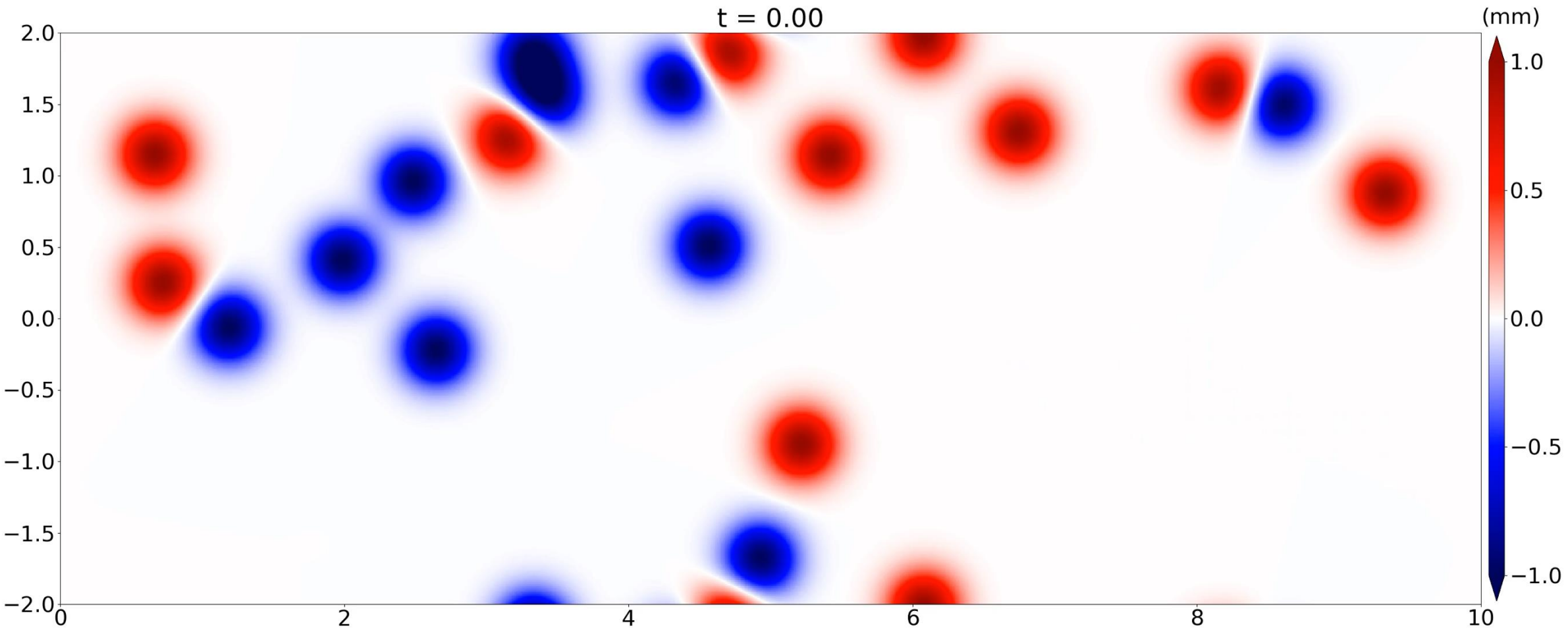

Homework 1

Homework 1 (deadline: Oct. 10)

Demonstrate barotropic instability numerically based on the shallow water quasi-geostrophic equation in the presence of a background zonal wind shear $U(y)$. You can build your own code based on the python code shown in the class (the python code "solve_2D_nonlinear_case1.ipynb" can be downloaded from the course website `https://qiuyang50.github.io/_pages/modeling_2024fall/`). The shallow water quasi-geostrophic equation reads as follows,

$$\frac{D}{Dt}\left(\nabla^2\psi - f^2F\psi\right) + \beta\frac{\partial\psi}{\partial x} = 0$$

where $\frac{D}{Dt} = \frac{\partial}{\partial t} - \frac{\partial\psi}{\partial y}\frac{\partial}{\partial x} + \frac{\partial\psi}{\partial x}\frac{\partial}{\partial y}$, f, F, β are all dimensionless constant, $U(y)$ has the following profile,

$$U(y) = \begin{cases} \frac{2-y}{b} & \text{if} \quad 2-b \le y \le 2 \\ 1 & \text{if} \quad a \le y < 2-b \\ \frac{y}{a} & \text{if} \quad -a \le y < a \\ -1 & \text{if} \quad b-2 \le y < -a \\ -\frac{y+2}{b} & \text{if} \quad -2 \le y < b-2 \end{cases}$$

where $b = 0.25$, a is a tunable parameter to determine the width of the wind shear in the middle.

Step 1: initialize the variable ψ. Hint: you can set the initial value of ψ as a combination of background state and a perturbation, $\psi(x, y, 0) = \Psi(y) + \psi'$, where $\Psi(y)$ satisfies $U(y) = -\frac{\partial\Psi(y)}{\partial y}$. You can use fast Fourier transform method (FFT) as we did in the python code to calculate $\Psi(y)$.

Step 2: add a perturbation ψ', which has to be small in amplitude and periodic at the domain boundaries. For example,

$$\psi' = 10^{-4}\sin\left(\frac{2\pi k}{L}x\right)e^{-\frac{y^2}{a^2}}$$

You may try other forms of perturbations.

Step 3: consider multiple scenarios with different values of a and k (e.g., $a = 0.5, k = 3$) and compare your results with the theoretical prediction mentioned in the class. Hint: $a * k$ should be small enough for the emergence of instability. See chapter 6.2 (page 256) in Vallis's book.

Homework requirement: please summarize all you findings in a report, particularly including several snapshots of the potential vorticity field $PV = \nabla^2\psi - f^2F\psi$ to demonstrate the barotropic instability. A thorough discussion about the choice of a and k in terms of barotropic instability is appreciated.

Tips: the whole simulation takes about 30 mins to finish. If you wish to store less output to save disk, just increase the value of the parameter "ngap" (solutions are saved every ngap steps).

淮地转模型应用实例

JGR Atmospheres

FEATURE ARTICLE
10.1029/2019JD030912

PV-Q Perspective of Cyclogenesis and Vertical Velocity Development Downstream of the Tibetan Plateau

Guoxiong Wu[1,2], Tingting Ma[1,3], Yimin Liu[1,2,4], and Zhihong Jiang[3]

[1]State Key Laboratory of Numerical Modeling for Atmospheric Sciences and Geophysical Fluid Dynamics (LASG), Institute of Atmospheric Physics (IAP), Chinese Academy of Sciences (CAS), Beijing, China, [2]College of Earth Science, University of Chinese Academy of Sciences, Beijing, China, [3]Key Laboratory of Meteorological Disaster of Ministry of Education (KLME)/Collaborative Innovation Center on Forecast and Evaluation of Meteorological Disasters (CIC-FEMD), Nanjing University of Information Science and Technology, Nanjing, China, [4]CAS Center for Excellence in Tibetan Plateau Earth Sciences, Beijing, China

青藏高原

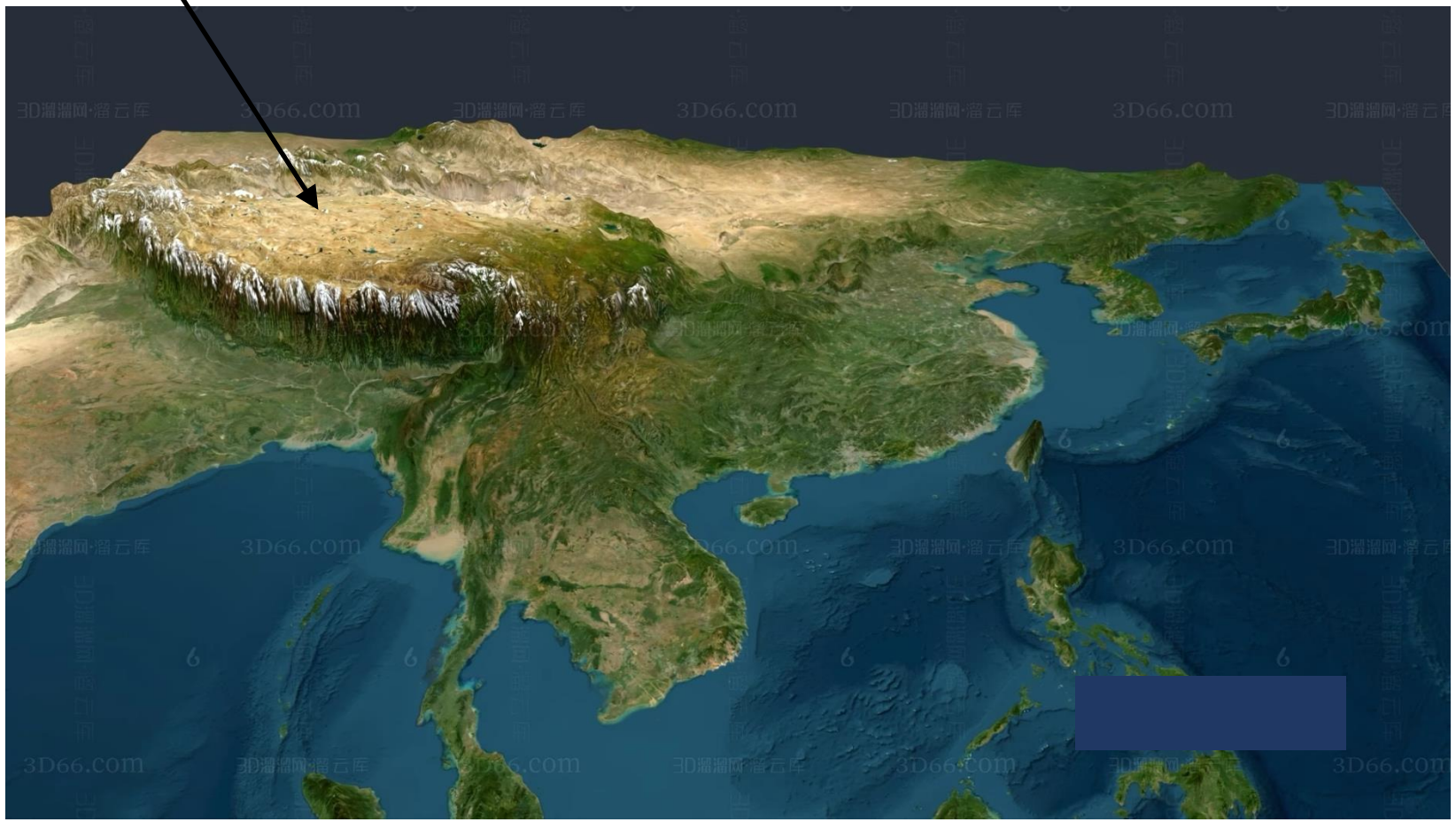

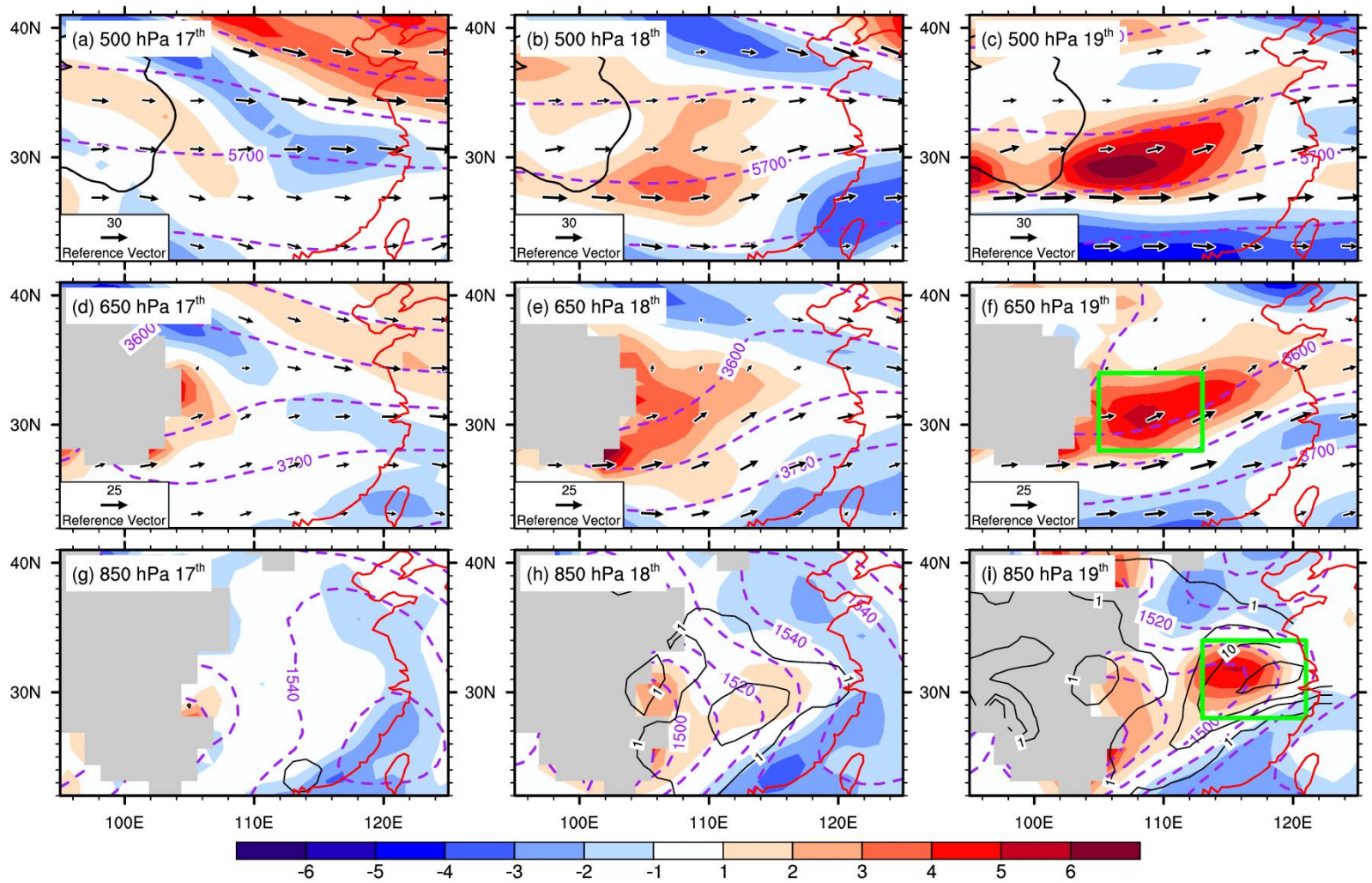

Figure 1. Distributions of daily mean relative vorticity (shading, 10^{-5} s^{-1}), geopotential height (purple dashed line, m), and wind (vector, m s^{-1}) at (a)–(c) 500 hPa, (d)–(f) 650 hPa, and (g)–(i) 850 hPa on 17 January (left column), 18 January (middle column), and 19 January 2008 (right column). Box area V (28°–34°N, 105°–113°E) in (f) denotes the key area of relative vorticity growth, and box area R (28°–34°N, 113°–121°E) in (i) denotes the key area of precipitation and vertical velocity. Black contour in (a)–(c) indicates the elevation of 3000 m. Gray area in (d)–(i) denotes the Tibetan Plateau. Black contours in (g)–(i) indicate daily precipitation of 1, 5, 10, and 20 mm.

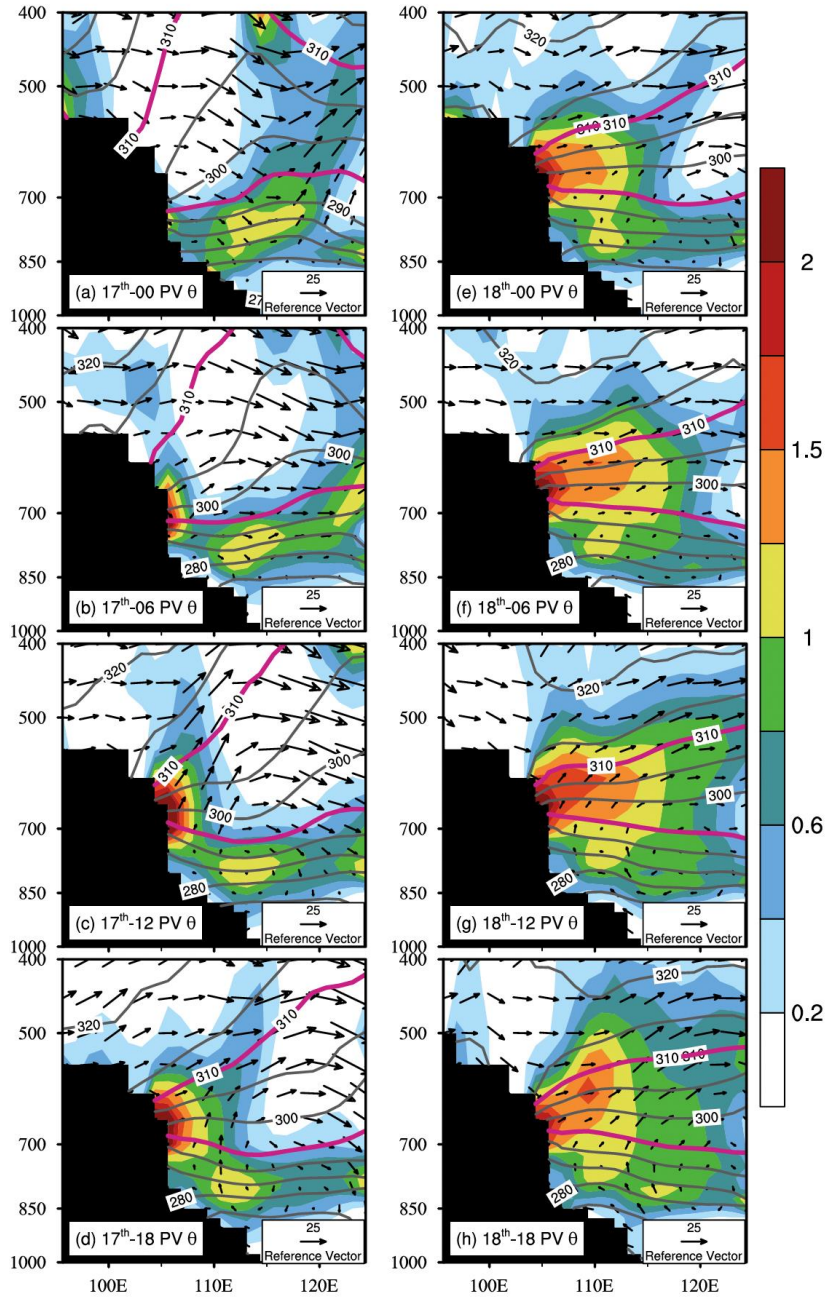

Figure 2. Vertical cross section along 33°N of PV (shading, PVU; 1 PVU = 10^{-6} K m^2 s^{-1} kg^{-1}), potential temperature (contour, K), and reanalysis wind ($u\,\vec{i} + \omega_{OB}\,\vec{k}$, vector, units: u in m s^{-1} and ω_{OB} in Pa s^{-1} [values multiplied by a factor of −50]) from (a) 00 UTC on 17 January to (h) 18 UTC on 18 January 2008 at 6-hr intervals. Heavy magenta contours denote isentropic temperature of 295 and 310 K.

PV theory has been used widely in dynamic analysis of weather systems, as reviewed in Hoskins et al. (1985). The celebrated hydrodynamic PV equation developed by Ertel (1942) is:

$$\begin{cases} \dfrac{dP}{dt} = \alpha\left[\vec{\zeta}_a \cdot \nabla\dot{\theta} + \nabla \times \vec{F} \cdot \nabla\theta\right] \\ P = \alpha\vec{\zeta}_a \cdot \nabla\theta \end{cases} \tag{4}$$

where α is specific volume, $\vec{\zeta}_a$ is 3-D absolute vorticity, $\vec{F}$ is 3-D frictional acceleration in the momentum equation, and ∇ is a 3-D gradient operator. The PV Equation 4 considers the impact of both diabatic

change in specific volume can also cause a change in W. In terrain-following hybrid σ-p coordinate

$$\sigma = (p - p_T)/(p_S - p_T),$$

the local change of W_σ becomes

$$\frac{\partial W_\sigma}{\partial t} = -\nabla_\sigma \cdot \left[\vec{V} W_\sigma - \vec{\zeta}_{a\sigma}\dot{\theta} - \theta\nabla_\sigma \times \vec{F_\sigma}\right], \tag{6}$$

(I) (II) (III)

$$W = \vec{\zeta}_a \cdot \nabla\theta$$

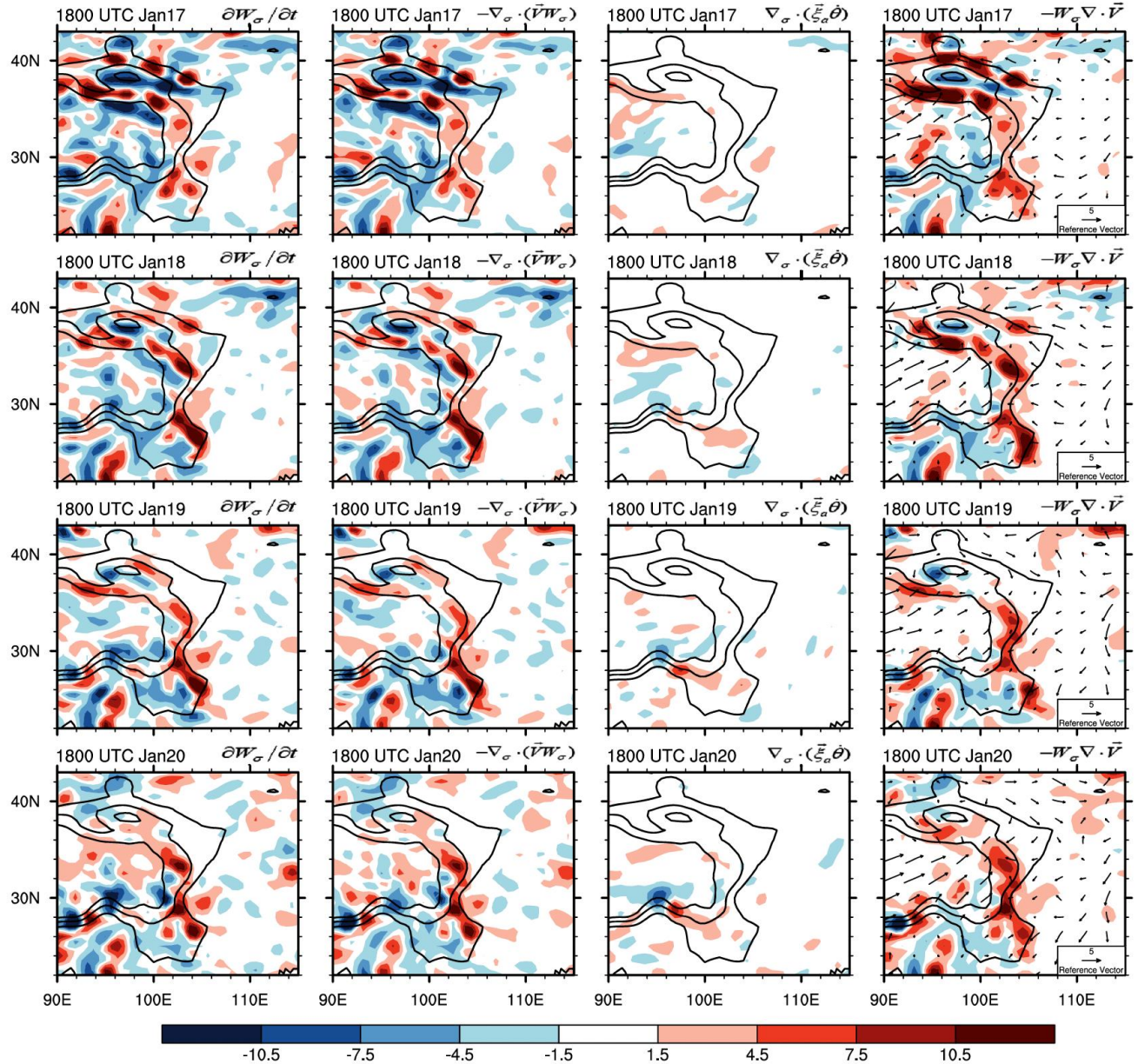

Figure 3. Distributions near the surface at 18 UTC of (left column) the tendency of surface potential vorticity density ($\partial W_\sigma/\partial t$), (second column) W-flux divergence term ($-\nabla_\sigma\cdot\left(\vec{V}W_\sigma\right)$), (third column) diabatic heating term ($\nabla_\sigma\cdot\left(\vec{\xi}_{a\sigma}\dot{\theta}\right)$), and (right column) divergence term ($-W_\sigma\nabla_\sigma\cdot\vec{V}$) and surface wind at 2 m (vector, m s^{-1}) from 17 January (top row) to 20 January (bottom row) 2008. Black contours indicate elevations of 1,500, 3,000, and 4,000 m. Unit in shading is 10^{-7} K s^{-2}.

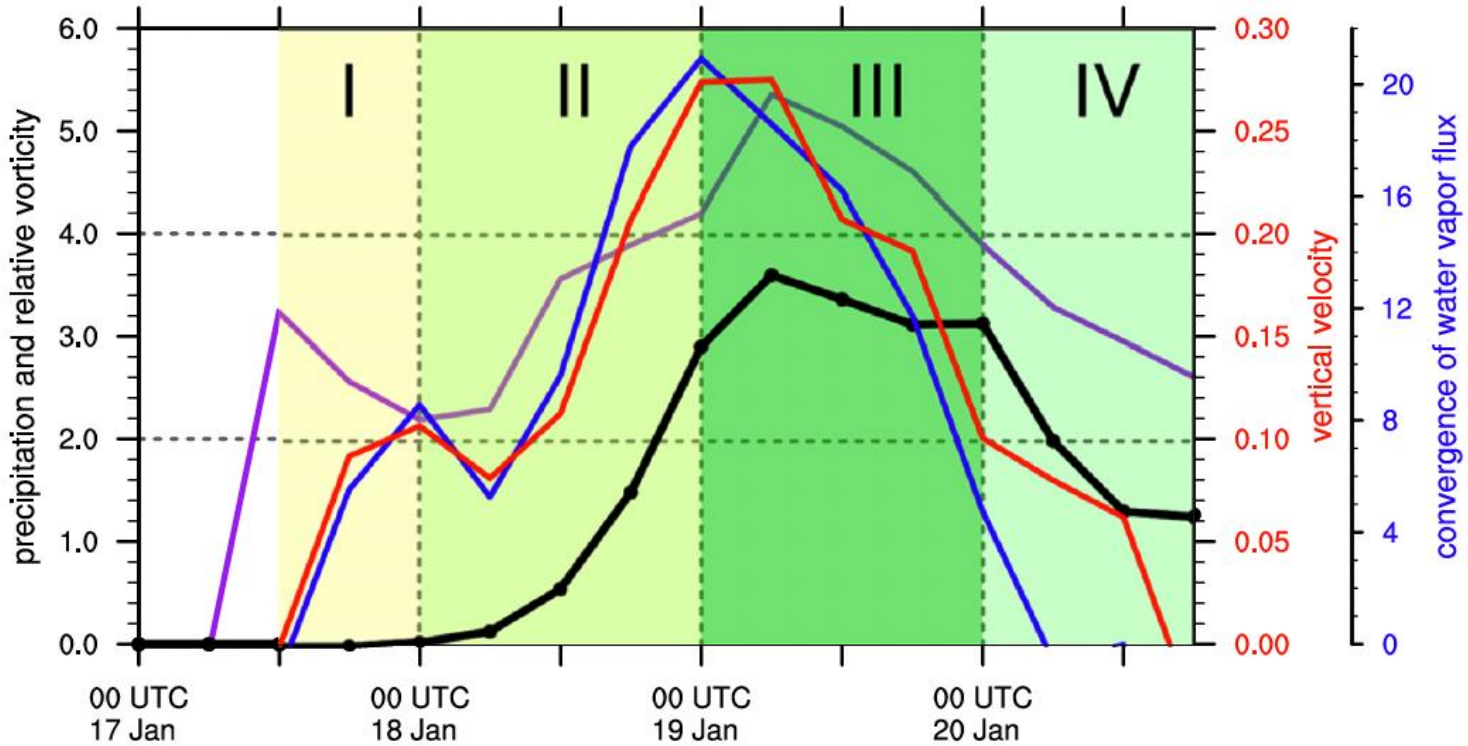

Figure 4. Evolution from 00 UTC 17 January to 18 UTC 20 January of the area-mean relative vorticity (purple curve, 10^{-5} s^{-1}) at 650 hPa averaged over box area V shown in Figure 1f; and the area-mean 6-hr accumulative precipitation (black curve, mm), vertical velocity (red curve, Pa s^{-1}; multiplied by a factor of −1) at 650 hPa, and vertical integral of convergence of water vapor flux from the surface to 650 hPa (blue curve, 10^{-7} kg m^{-2} s^{-1}; multiplied by a factor of −1) averaged over box area R shown in Figure 1i.

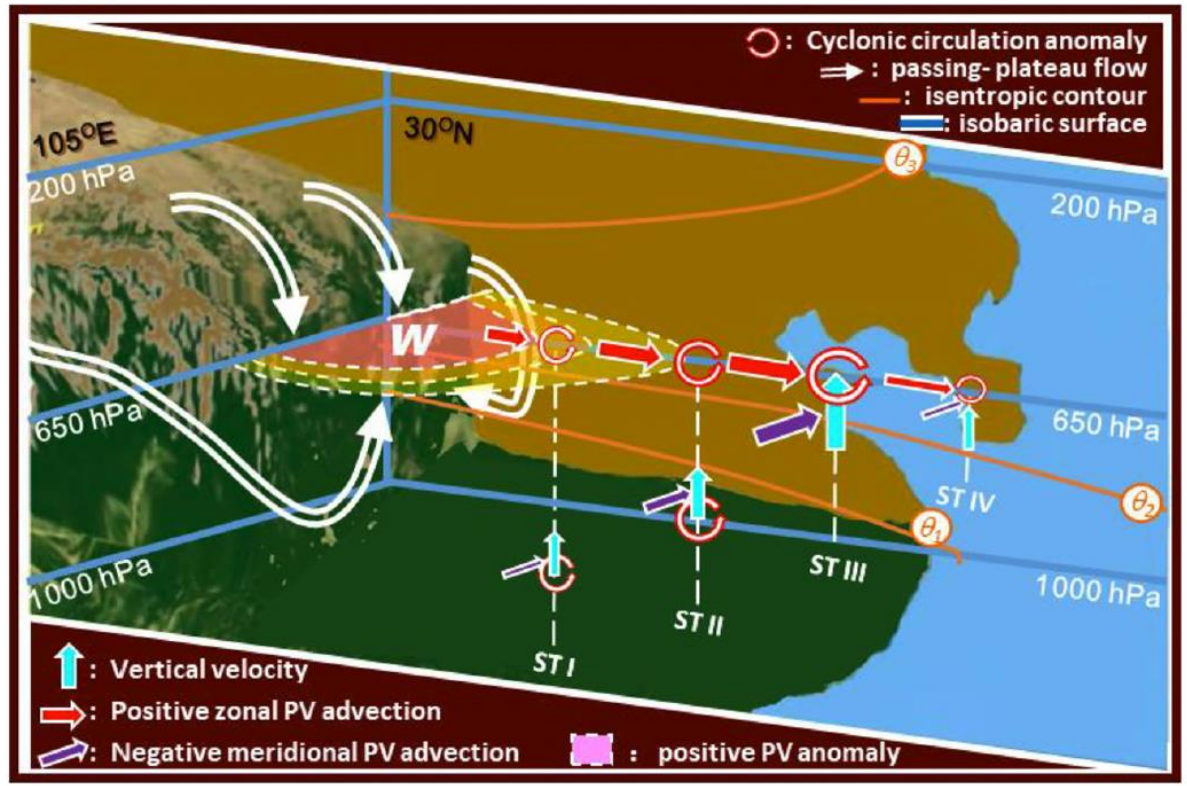

Figure 12. Schematic of PV restructuring in the region of the Tibetan Plateau (TP) and the impact of PV advection on downstream circulation during different stages (ST) of cyclogenesis. Stage I: Surface airflow convergence in the lee of the TP increases local PV density *W*, generating a positive relative vorticity anomaly and initiating light rain near the TP. Stage II: Eastward moving positive vorticity anomaly is intensified owing to reduced static stability. Positive zonal PV advection in the midtroposphere and increased southerly and negative meridional PV advection below enhances cyclogenesis, air ascent, and precipitation. Stage III: Negative meridional PV advection is located immediately below the center of strong positive zonal PV advection, and cyclonic vorticity, vertical velocity, and precipitation are peaked. Stage IV: Negative meridional PV advection tends to overlay the positive center of zonal PV advection. Consequently, the cyclone and air ascent are both weakened, and precipitation is diminished.

相关课程推荐

《流体力学》

丁峰

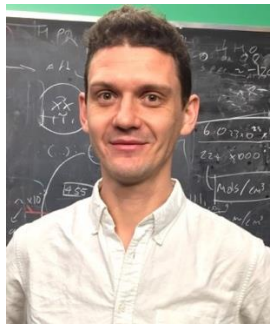

Daniel Koll

《大气动力学基础》

聂绩

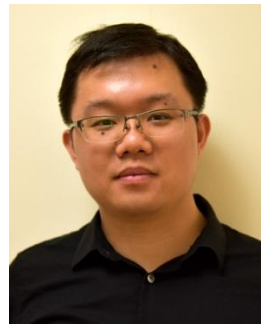

杨邱

《数值天气预报》

孟智勇

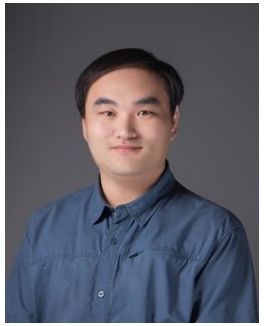

闻新宇